A novel high voltage LIGBT with an n-region in p-substrate*

Cheng Jianbing(成建兵)[1,†], Zhang Bo(张波)[2], and Li Zhaoji(李肇基)[2]

[1]School of Electronic Science & Engineering, Nanjing University of Posts and Telecommunications, Nanjing 210003, China
[2]State Key Laboratory of Electronic Thin Films and Integrated Devices, University of Electronic Science and Technology of China, Chengdu 610054, China

Abstract: A novel 4 μm thickness drift region lateral insulated gate bipolar transistor with a floating n-region (NR-LIGBT) in p-substrate is proposed. Due to the field modulation from the n-region, the vertical blocking capability is enhanced and the breakdown voltage is improved significantly. Low area cost, high current capability and short turn-off time are achieved because of the high average electric field per micron. Simulation results show that the blocking capability of the new LIGBT increases by about 58% when compared with the conventional LIGBT (C-LIGBT) for the same 100 μm drift region length. Furthermore, the turn-off time is shorter than that of the conventional LIGBT for nearly same blocking capability.

Key words: NR-LIGBT; blocking capability; current capability; turn-off time
DOI: 10.1088/1674-4926/32/11/114003 **EEACC:** 2560

1. Introduction

In power integrated circuits (PICs), lateral power devices (mainly lateral DMOST and IGBT) are key elements[1,2]. The LDMOST is widely applied in low voltage PIC because of the high switching speed. At the same time, the high on-resistance of the LDMOST at high breakdown voltage makes high power losses, which are unacceptable at high voltage applications. For high voltage PICs, the LIGBT is a promising power device due to a simple gate drive structure and low forward voltage drop[3]. The low forward voltage drop results from conductivity modulation in drift region at on-state and the modulation can be enhanced by decreasing n-buffer concentration. However, a low n-buffer concentration will cause low vertical punch-through voltage in junction isolation (JI) technology[4]. So, to achieve virtues of the thin drift LIGBT, the vertical breakdown voltage should be improved firstly.

We have presented the LDMOST with floating n-region previously[5−7]. In this paper, we propose a novel LIGBT with a partly floating n-region. The thickness of the drift region is only 4 μm. The performances at blocking and turn-off states are compared between the new and the conventional structures. Simulation results show that for the new structure, higher blocking voltage and higher turn-off speed are achieved.

2. Device structures and off-state operation

Figures 1 and 2 show the cross-sections of the conventional LIGBT structure and the novel counterpart, respectively. Both of the structures have a p-buried-layer under the p-body[8]. The difference between both devices is that a floating n-region is embedded in the p-substrate of the NR-LIGBT. The n-region helps to improve the blocking capability because of the optimum field distribution of the novel structure. Furthermore, due to the high average field of the new device, smaller area is needed and then the less stored holes for given breakdown voltage. As a result, the turn-off performance of the new structure is improved. The simulation results in this paper are achieved by the device simulator MEDICI[9] and the device parameters in simulation are listed in Table 1.

The vertical electric field distribution of the proposed LIGBT at breakdown is compared with that of the conventional one in Fig. 3. The electrodes of the source, the gate and the substrate are contacted with 0 V. For the conventional LIGBT, there are only one field peak at the p-substrate/n-drift junction and two peaks for the proposed device at the p-substrate/n-region and the p-substrate/n-drift junctions. Premature breakdown is apt to occur in the conventional LIGBT. However, for the new structure, there is another field peak caused by the extra

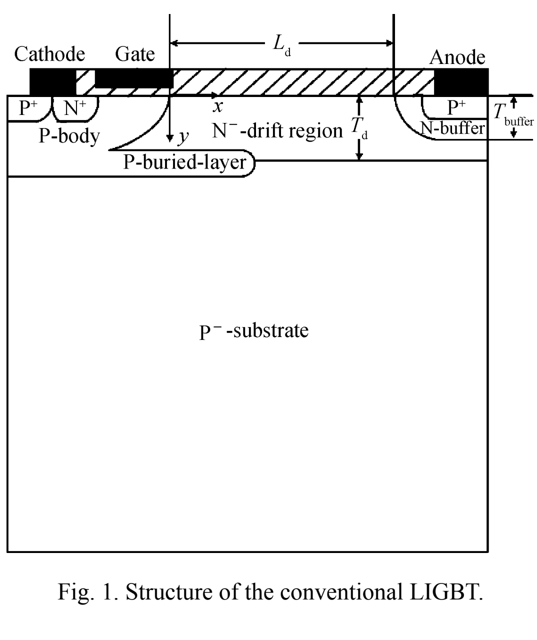

Fig. 1. Structure of the conventional LIGBT.

* Project supported by the National Natural Science Foundation of China (No. 61076082).
† Corresponding author. Email: chengjianbing08@yahoo.com.cn
Received 3 May 2011, revised manuscript received 18 July 2011

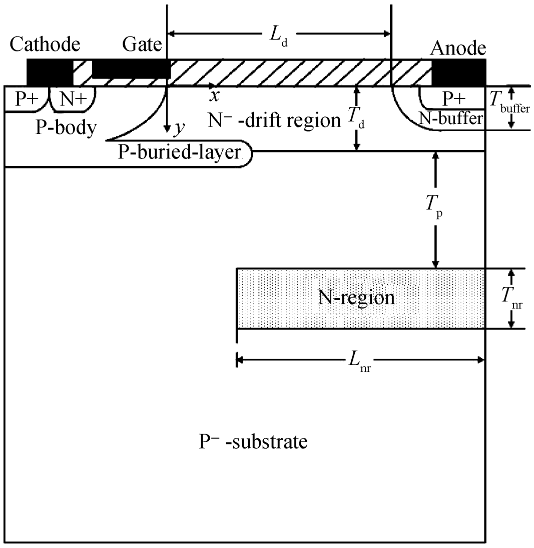

Fig. 2. Structure of the proposed NR-LIGBT.

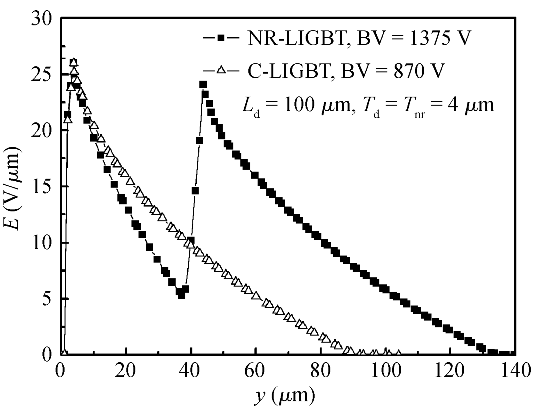

Fig. 3. Vertical electric field distributions at breakdown.

Table 1. Device parameters in simulation.

Device parameter	Value
Drift region thickness, T_d	4 μm
N-region thickness, T_{nr}	4 μm
N-buffer junction depth, T_{buffer}	2 μm
Distance from the n-region to the drift region, T_p	35 μm
N-buffer-layer doping concentration, N_{buffer}	5×10^{17} cm^{-3}
P-substrate doping concentration, N_{sub}	1×10^{14} cm^{-3}

space charges in the n-region in blocking-state and the vertical breakdown voltage is improved significantly. As a result, for given same 100 μm drift region length, the breakdown voltage of the new device is increased from 870 to 1375 V in comparison with that of the conventional one.

Figure 4 compares the surface electric field distributions of the conventional and the proposed LIGBT when the breakdown occurs. There are three field peaks, two are at the edge of the drift region and another is at the end of the p-buried-layer. The field modulation from the n-region in the substrate improves the conventional low field at the middle drift region. Seen from this figure, the average field per micron of the proposed device is significantly higher than that of the conventional one. As a result, less device area of the new structure is needed for the given breakdown voltage.

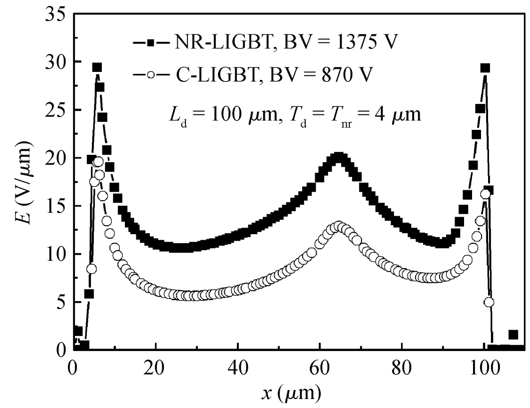

Fig. 4. Surface electric field distributions at breakdown.

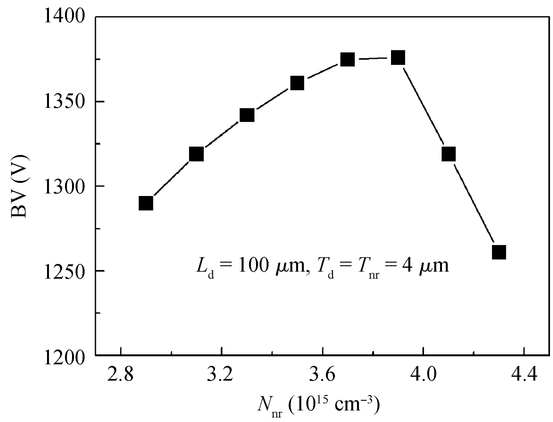

Fig. 5. Influence of the n-region doping concentration on the breakdown voltage.

The relationship between the breakdown voltage and the n-region doping concentration is shown in Fig. 5. There is an optimum doping concentration (N_{opt}, 3.9×10^{15} cm^{-3}) and the breakdown voltage is highest at this point. Also seen from the figure, the curve is not symmetric. That is to say, the intensity of field modulation is different for different area. At the gate side, the modulation density is soft and it is strong at the anode side. When the doping concentration is higher than the N_{opt}, the breakdown occurs at the gate edge. Conversely, the breakdown occurs at the anode edge. So, the breakdown voltages decrease slowly when the n-region doping concentrations are less than the optimum value. When the concentrations are more than the optimum value, the breakdown voltages decrease sharply.

Figure 6 shows relationship between the breakdown voltage and the drift region length. For the conventional LIGBT, the breakdown voltage increases slowly with the drift length increasing. However, for the proposed device, the blocking capability improves rapidly and the slope of the line is nearly equal to 14 V/μm. The blocking capability improvement results from the vertical breakdown voltage improvement from the n-region in the p-substrate.

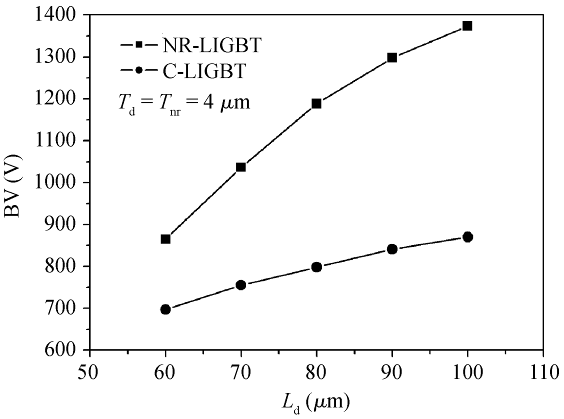

Fig. 6. Relationship between the breakdown voltage and the drift region length.

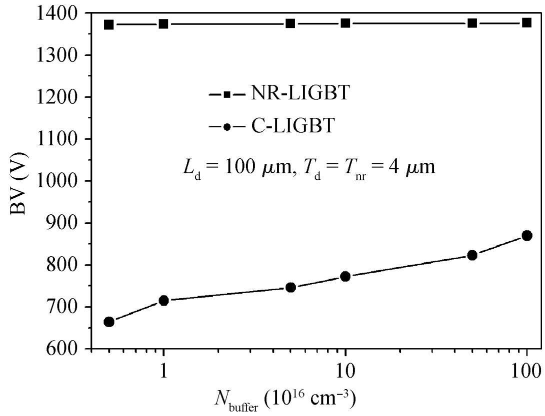

Fig. 8. Relationship between the breakdown voltage and n-buffer doping concentration.

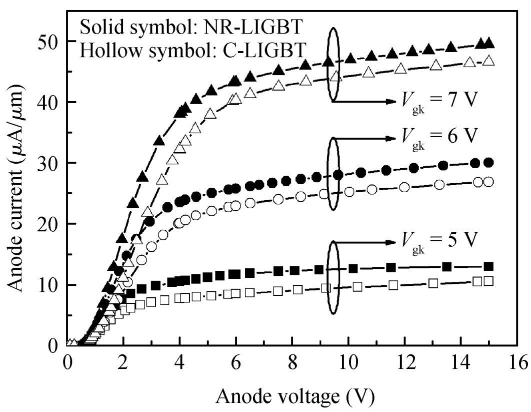

Fig. 7. Relationship between the anode current and voltage.

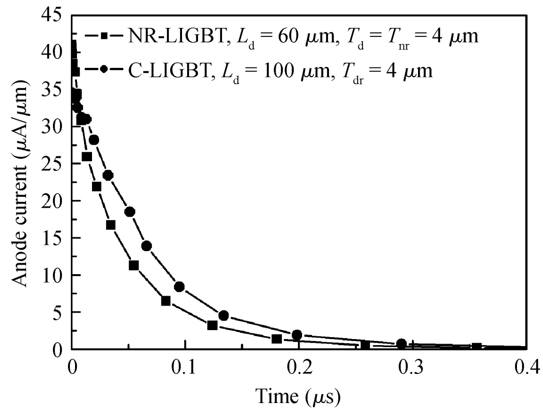

Fig. 9. Turn-off waveforms of the C-LIGBT and the NR-LIGBT.

3. On-state and turn-off characteristics

In this paper, the on-state and the turn-off characteristics are simulated under the condition of nearly same blocking capabilities. The breakdown voltage of the new device is 895 V and that of the conventional one is 870 V. However, for the new structure, the drift lengths are 60 μm and 100 μm of the conventional device, which is because the average field of the proposed LIGBT is higher from Fig. 4.

The forward conduction characteristic is explained by the bipolar/MOSFET model. The anode current can be expressed as[3]

$$I_{\text{anode}} = \frac{I_{\text{MOS}}}{1 - \alpha_{\text{PNP}}}, \tag{1}$$

$$\alpha_{\text{PNP}} = \frac{1}{\cosh[(L_{\text{d}} - L_{\text{dep}})/L_{\text{a}}]}, \tag{2}$$

$$I_{\text{anode}} = \frac{I_{\text{MOS}}}{1 - \{\cosh[(L_{\text{d}} - L_{\text{dep}})/L_{\text{a}}]\}^{-1}}, \tag{3}$$

where I_{anode} is the anode current, I_{MOS} is the electron current through the MOSFET, α_{PNP} is the current gain of the lateral PNP transistor, L_{dep} is the width of the depleted drift region and L_{a} is the diffusion length, respectively. The optimum drift doping concentrations of the conventional and the proposed LIGBT are almost same. At on-state, the depleted drift widths are almost not change when the anode voltages of the two structures are equal. So, from Eq. (3), the anode current of the proposed LIGBT is higher and then higher current capability because of the shorter drift region length. The output characteristics of the two LIGBTs are compared in Fig. 7. Solid lines show performance of the new LIGBT and hollow lines show performance of the conventional one. The drift length and the breakdown voltage of the NR-LIGBT are 60 μm and 895 V, and 100 μm and 870 V of the C-LIGBT. It is clear that the anode current of the NR-LIGBT is higher for the same gate and anode voltages at on-state.

Figure 8 shows the relationship between the breakdown voltage and the n-buffer doping concentration. For the NR-LIGBT, the breakdown voltage nearly does not change with increasing the n-buffer doping concentration. The breakdown voltage increases for the C-LIGBT. When the concentration is less than 1×10^{19} cm^{-3}, it is punch-through breakdown and the electron ionization coefficient is less than 1 for the C-LIGBT. For the NR-LIGBT, the coefficient is always larger than 1 from 5×10^{16} to 1×10^{19} cm^{-3} and the breakdown is avalanche breakdown. So, the process tolerance of the n-buffer doping of the NR-LIGBT is superior to that of the C-LIGBT.

The LIGBT is suffered from slow turn-off time because of the "current tail" or high concentration of minority carriers in the drift region and the substrate after the device has been turned off[3]. Figure 9 shows the turn-off waveforms of the proposed and the conventional LIGBT with a resistive load. The carrier-lifetimes are 1 μs and the temperature is 300 K. Gate turn-off (from $V_g = 5$ to 0 V in 10 ns) has been simulated with the resistive load of 1×10^4 Ω and an off-state anode voltage of 15 V. The shorter drift region, the less minority carriers are stored for same drift doping concentrations. This explains the short turn-off time of the proposed structure.

4. Conclusions

In this paper, a new LIGBT with the floating n-region has been presented. Because of the improvement of the vertical breakdown voltage and the less stored minority carriers, the new structure shows less device area, higher breakdown voltage and shorter turn-off time. For the same 100 μm drift length, the breakdown voltage increases from 870 V of the conventional LIGBT to 1375 V.

References

[1] Zhu R, Khemka V, Bose A, et al. Stepped-drift LDMOSFET: a novel drift region engineered device for advanced smart power technologies. Proceedings of the 18th International Symposium on Power Semiconductor Devices & IC's, 2006: 1

[2] Bakeroot B, Doutreloigne J, Vanmeerbeek P, et al. Analysis of a narrow-base lateral IGBT with double buried layer for junction-isolated smart-power technologies. IEEE Trans Electron Devices, 2008, 55(1): 435

[3] Baliga B J. Power semiconductor devices. PWS Publishing Company, 1996

[4] Hardikar S, Tadikonda R, Sweet M, et al. A fast switching segmented anode NPN controlled LIGBT. IEEE Electron Device Lett, 2003, 24(11): 701

[5] Cheng Jianbing, Zhang Bo, Li Zhaoji. Breakdown voltage characteristics of LDMOS with a full depletion floating buried layer. Chinese Journal of Semiconductors, 2008, 29(2): 344

[6] Cheng J B, Zhang B, Li Z J. A novel 1200-V LDMOSFET with floating buried layer in substrate. IEEE Electron Device Lett, 2008, 29(6): 645

[7] Cheng J B, Zhang B, Li Z J. Longitudinal junction termination technique by multiple floating buried-layers for LDMOST. Electron Lett, 2008, 44(15): 933

[8] Stupp E H, Colak S, Ni J. Low specific on-resistance 400 V LDMOST. IEDM, 1981: 426

[9] TMA MEDICI 4.2, Technol Modeling Assoc, Inc, Palo Alto, CA, 1998